

Article

Microwave-Promoted Total Synthesis of Puniceloid D for Modulating the Liver X Receptor

Young Jin Jung ^{1,†}, Narges Hosseinasab ^{2,†} , Jungjin Park ², Soonsil Hyun ² , Jae-Kyung Jung ² 
and Jae-Hwan Kwak ^{1,2,*} ¹ College of Pharmacy, Kyungsung University, Busan 48434, Republic of Korea; louisj0750@naver.com² College of Pharmacy, Chungbuk National University, Cheongju 28160, Republic of Korea; nargeshosseini@chungbuk.ac.kr (N.H.); jjpark0823@chungbuk.ac.kr (J.P.); shyun@chungbuk.ac.kr (S.H.); orgjkjung@chungbuk.ac.kr (J.-K.J.)

* Correspondence: jhkwak@chungbuk.ac.kr; Tel.: +82-43-261-2997

† These authors contributed equally to this work.

Abstract: A growing global health concern is metabolic syndrome, which is defined by low HDL, diabetes, hypertension, and abdominal obesity. Nuclear receptors are attractive targets for treatment of diseases associated with metabolic syndrome. Liver X receptors (LXRs) have become one of the most significant pharmacological targets among nuclear receptors. Multiple research studies emphasize the essential function of the liver X receptor (LXR) in the pathophysiology of metabolic syndrome. Puniceloid D, among natural products, demonstrated promising effects on LXR α . However, attempts at the total synthesis of natural products were faced with challenges, including long synthetic steps and low yields, requiring a more efficient approach. In this study, for the first time, we successfully synthesized puniceloid D through a seven-step process and conducted docking studies to gain a comprehensive understanding of the interactions involved in the binding of puniceloid D to LXR within different heterodimeric contexts. Our understanding of the pathophysiology of metabolic syndrome could be improved by these findings, which might assist with the development of novel treatment strategies.

Keywords: liver X receptors; nuclear receptor; puniceloid D; total synthesis; natural products

Citation: Jung, Y.J.; Hosseinasab, N.; Park, J.; Hyun, S.; Jung, J.-K.; Kwak, J.-H. Microwave-Promoted Total Synthesis of Puniceloid D for Modulating the Liver X Receptor. *Molecules* **2024**, *29*, 416. <https://doi.org/10.3390/molecules29020416>

Academic Editors: Shao-Hua Wang, Xuetao Xu and Xi Zheng

Received: 19 December 2023

Revised: 9 January 2024

Accepted: 14 January 2024

Published: 15 January 2024



Copyright: © 2024 by the authors. Licensee MDPI, Basel, Switzerland. This article is an open access article distributed under the terms and conditions of the Creative Commons Attribution (CC BY) license (<https://creativecommons.org/licenses/by/4.0/>).

1. Introduction

One of the major obstacles for health systems worldwide is the diseases associated with metabolic syndrome. The condition consists of several risk factors, particularly linked to diabetes and cardiovascular disease. The cluster of metabolic factors includes low HDL cholesterol, high triglyceride levels, impaired fasting glucose, high blood pressure, and abdominal obesity [1]. Therefore, the management and treatment of metabolic syndrome are of highest priority. Recent study data indicate that nuclear receptors play a critical role in the pathophysiology of this condition [2].

Target gene expression in a wide range of physiological pathways, including metabolic processes, is regulated by nuclear receptors, which are ligand-activated transcription factors [3–5]. Nuclear receptors associated with metabolism are categorized as type 2 nuclear receptors, which are found inside the nucleus regardless of ligand binding [6]. Liver X receptors (LXR α (NR1H3) and LXR β (NR1H2)), farnesoid X receptor (FXR, NR1H4), peroxisome proliferator-activated receptors (PPARs, NR1C1/NR1C2/NR1C3), and RXRs are examples of type 2 nuclear receptors for the regulation of metabolic processes. Fatty acids, oxysterols, bile acids, and retinoids are ligands for these receptors, highlighting their importance in the control of metabolic pathways [7,8].

An essential role for liver X receptors is to regulate innate immunity, inflammatory responses, and lipid and cholesterol metabolism [9–11]. There are two isoforms of the liver X receptor: LXR α and LXR β [12]. While LXR β (NR1H2) is expressed everywhere, LXR α

(NR1H3) is expressed in metabolically active tissues such as the liver, adipose, kidney, macrophages, and intestines [13,14]. LXR inhibits gluconeogenesis, promotes bile secretion, raises cholesterol clearance in the liver, suppresses the macrophage inflammatory response, increases clearance of cholesterol in the small intestine, and facilitates glucose reabsorption into cells by promoting the expression of GLUT4 (glucose transporter type 4) in adipose tissue [15]. In addition to their role in regulating lipid metabolism, LXRs play a crucial role in controlling blood sugar levels by modulating glucose transport proteins such as GLUT4/5, and regulatory proteins like ChREBP (carbohydrate responsive element-binding protein), which are involved in glucose homeostasis [16]. Therefore, the majority of the research performed to identify LXR modulators with therapeutic potential has focused on the development of LXR agonists [17,18].

The search for LXR modulators for the treatment of metabolic diseases is ongoing. Utilizing natural products that potentially offer decreased potency and fewer side effects or demonstrate tissue- or subtype-selective activity represents a viable approach [1]. Figure 1 displays some discovered LXR α agonists derived from natural products (marine-derived fungi) [19]. Based on a study by Liang et al., [19] puniceloid C and D were identified as the most potent LXR α agonists.

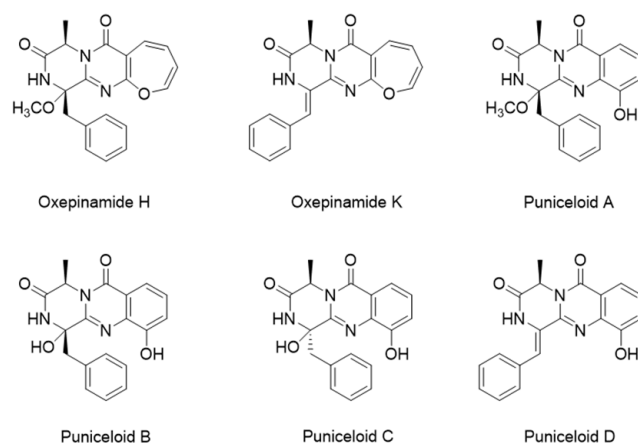


Figure 1. Structures of natural product-oriented LXR α agonists.

Quinazolinones are known for their diverse and significant biological properties, including cholinesterase inhibition and antitumor, antiviral, anti-inflammatory, anticancer, and protein kinase inhibitory effects [20]. The presence of quinazolinone and its derivatives is noted in over 100 naturally occurring alkaloids, comprising a crucial class of fused heterocycles [21]. Several families of alkaloids are represented by fungal quinazolinone metabolites that contain the core pyrazino[2,1-*b*]quinazoline-3,6-dione (A) scaffold [22].

Scaffold A is a structural motif found in several natural products known for their notable biological activities, such as glyantripine (B), fiscalin B (C), fumiquinazolines F (D) and G (E), as well as puniceloids A–D (Figure 2).

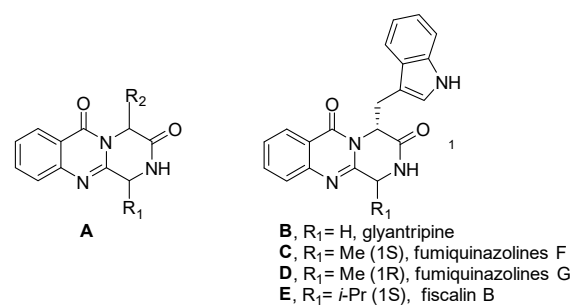


Figure 2. Natural products containing pyrazino[2,1-*b*]quinazoline-3,6-dione (A).

Derivatives of this system have been synthesized using three distinct methods: the cyclization of 4(3*H*)-quinazolinones (a), the cyclocondensation of 2,5-piperazinediones and anthranilic acid derivatives (b), and the use of open-chain tripeptides, with anthranilic acid positioned at the C-terminal (c1), N-terminal (c2), or as the intermediate residue (c3) [23] (Figure 3).

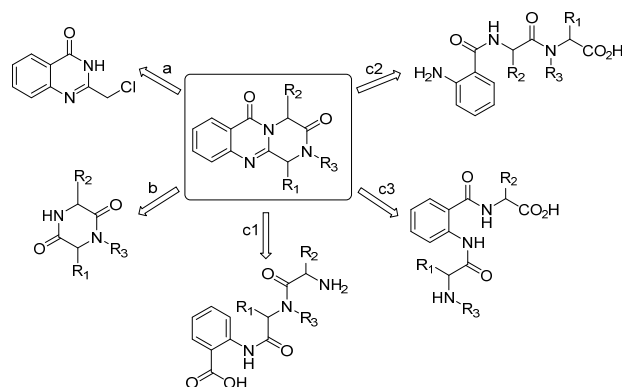


Figure 3. Different synthetic approaches to the parent ring system (pyrazino[2,1-*b*]quinazoline-3,6-dione).

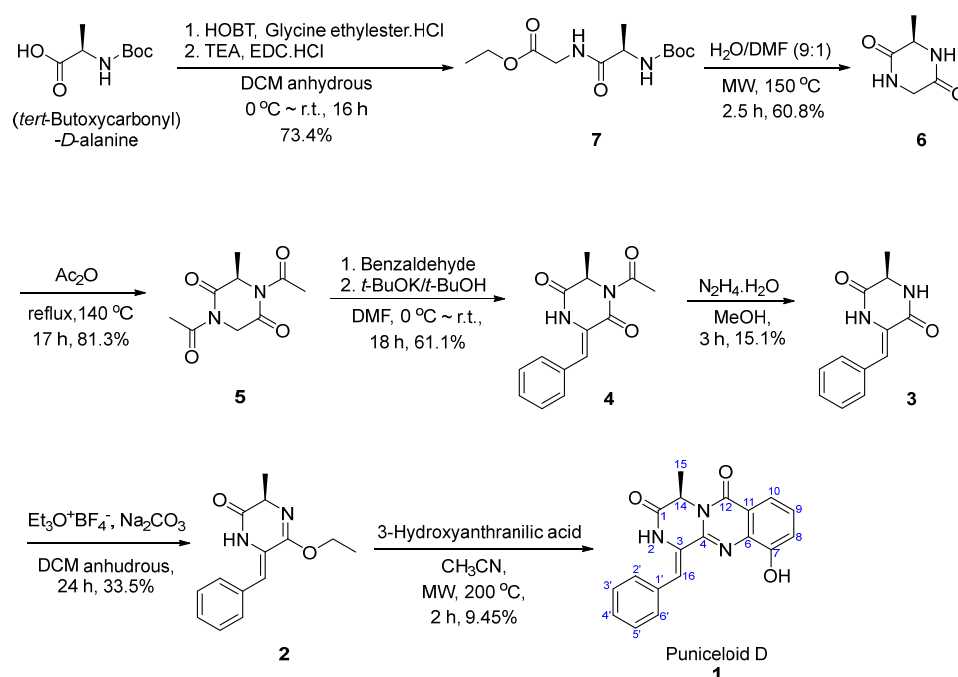
Considering the increasing interest in natural products as potential sources of novel drugs [24] or as lead structures for drug discovery in medicinal and organic chemistry [25,26], and drawing inspiration from existing data [19] highlighting puniceloid D as the most potent LXR α agonist, our study presents the total synthesis of puniceloid D for the first time. Furthermore, significant results from molecular docking studies were obtained with puniceloid D.

2. Results

Total Synthesis of Puniceloid D

The first total synthesis of puniceloid D (1) involved seven steps. In our study, we chose route (b) (Figure 3) based on literature findings, as protecting N-2 was reported to enhance reactivity and prevent racemization [27]. In the first step, the reaction of (*tert*-butoxycarbonyl)-*D*-alanine with glycine ethyl ester hydrochloride as a nucleophile produced ethyl (*tert*-butoxycarbonyl)-*D*-alanyl-glycinate (7) at a 73.4% yield. This reaction was facilitated by using EDC and HOBT, which convert amine to amide [28]. According to the literature, the stereochemistry is preserved [29,30]. In the second step, intramolecular cyclization occurred under microwave conditions, involving the removal of the Boc group. Subsequently, intramolecular nucleophilic addition of the amine in compound 7 to the carbonyl group, followed by the elimination of the ethoxy group, produced compound 6 [31]. The literature states that compound 6 was obtained with complete retention of the original stereochemical configuration of 7 through the use of HPLC analysis on the chiral phase [31]. Next, compound 6 was heated under reflux conditions in acetic anhydride to yield compound 5. Classically, an excess of acetic anhydride is used in solvent-free acetylation reactions and it preserves the stereochemistry [32]. To facilitate base-catalyzed condensation with aldehydes, compound 5 was diacetylated in the previous step. At room temperature, an aldol reaction is carried out between compound 5 and benzaldehyde, in the presence of potassium *t*-butoxide and DMF as a solvent, to form compound 4 [27]. The acetyl group reduces the pKa of the alpha carbonyl, making it easily deprotonated. Based on existing research, compound 4 maintains its stereochemical integrity [27,33]. Challenges in *E/Z* isomer selectivity could arise depending on the location of the phenyl ring. However, in the literature, the absence of NOE enhancement in vinyl protons upon N-H signal irradiation confirmed the *Z* configuration [27,34]. Compound 4 was deacetylated through treatment with hydrazine monohydrate, resulting in the formation of compound 3 [27]. The

removal of the acetyl group increased the polarity of the compound, making it less soluble in commonly used solvents such as ethyl acetate and dichloromethane. The reaction of compound **3** with Meerwein's salt (triethyloxonium tetrafluoroborate) in the presence of sodium carbonate resulted in the formation of the monoiminoether compound (**2**) [28,31]. Meerwein's salt can act as an alkylating agent by serving as a source of ethyl groups ($C_2H_5^+$) [35]. In accordance with published research [36], thermal treatment of compound **3** does not cause any changes to the stereocenter, leading to compound **2**. Despite the reaction running for 24 h, the yield was low because the starting material for this reaction was diketopiperazine, which has low reactivity. The number of equivalents of the Meerwein's salt was increased to enhance the yield, but when 2.2 equivalents were used, it was discovered that ethylation occurred on both carbonyl oxygens in the diketopiperazine ring, highlighting the importance of controlling the number of equivalents. Finally, compound **2** interacts with 3-hydroxyanthranilic acid under microwave conditions at 200 °C, followed by cyclization and elimination of hydroxy, resulting in the formation of puniceloid D (**1**) [37] (Scheme 1). In the literature, certain research groups have focused on producing 1-aryl methylene pyrazino[2,1-*b*]quinazoline-3,6-diones, which share similarities with puniceloid D. Cledera et al. detailed a seven-step synthesis of (*R,Z*)-1-(4-methoxybenzylidene)-4-methyl-1,2-dihydro-6*H*-pyrazino[2,1-*b*]quinazoline-3,6(4*H*)-dione under heating conditions at 120 °C for 2 h, achieving a 15% yield [27]. The same group also employed a 9-min microwave irradiation reaction, obtaining the same compound at a 26% yield [36]. Taking inspiration from this, we successfully synthesized puniceloid D (**1**) for the first time with a 9.45% yield, utilizing 3-hydroxyanthranilic acid under microwave irradiation for 2 h.



Scheme 1. Total synthesis of puniceloid D (**1**).

The ¹H NMR and ¹³C NMR spectra of the final synthesized compound (**1**) exhibited a complete match with the reported ones [19] (Table 1) (Figure S15).

Table 1. Comparative NMR (^1H (400 MHz) and ^{13}C (100 MHz)) analysis of the synthesized puniceloid D (**1**) and the reported results.

Position	Synthesized		Reported [19]	
	δ_{C} , Type	δ_{H} (J in Hz)	δ_{C} , Type	δ_{H} (J in Hz)
1	166.3	data	166.6, C	
2-NH		10.56, s		10.52, s
3	125.9		126.0, C	
4	143.3		144.1, C	
6	135.6		136.1, C	
7	151.7		152.8, C	
7-OH		9.76, s		9.75, s
8	117.8	7.26, dd (7.9, 1.4)	118.4, CH	7.26, dd (8.0, 1.0)
9	128.6	7.37, t (7.9)	128.1, CH	7.35, t (8.0)
10	116.3	7.58, dd (7.9, 1.4)	116.0, CH	7.58, dd (8.0, 1.0)
11	120.4		120.4, C	
12	160.0		159.5, C	
14	52.0	5.22, q (6.8)	51.2, CH	5.22, q (7.0)
15	19.5	1.49, d (7.0)	18.2, CH ₃	1.50, d (7.0)
16	117.7	7.71, s	117.2, CH	7.74, s
1'	133.0		134.0, C	
2',6'	129.2	7.66, d (7.71)	129.4, CH	7.65, d (7.5)
3',5'	128.7	7.47, t (7.62)	128.7, CH	7.47, t (7.5)
4'	129.7	7.37, m	127.6, CH	7.37, m

3. Discussion

According to the literature [19], the transactivation effects of puniceloid D and oxepinamide K on LXR α were investigated. Puniceloid D exhibited significant transcriptional activation on LXR α , demonstrating an EC₅₀ value of 1.7 μM . In contrast, oxepinamide K, which contains an oxepin unit, showed 29 times less active transcriptional activation on LXR α , with EC₅₀ values of 50 μM compared to puniceloid D. These findings indicate that the quinazolinone skeleton found in puniceloid D is essential in determining the observed bioactivity in the context of LXR α transactivation [38]. To enhance our understanding of the binding modes of puniceloid D and oxepinamide K with LXRs, we conducted molecular docking studies (in silico) using Glide in Extra Precision (XP), as implemented in Schrödinger (version 2023-4). The docking studies were performed with LXR α in the context of two different LXR α -RXR β and LXR α -RXR α LBD heterodimers, represented by PDB IDs 1UHL and 2ACL, respectively.

In our in silico docking study, we investigated the interactions of puniceloid D and oxepinamide K with two LXR α LBD (PDB ID 1UHL and PDB ID 2ACL). Puniceloid D notably exhibited π - π stacking interactions with Tyr32 and Phe257 when docked with LXR α from the LXR α -RXR β heterodimer (Figure 4). Similarly, in the docking study with LXR α from the LXR α -RXR α heterodimer, puniceloid D displayed π - π stacking interactions with Phe313 and hydrogen bonding interactions with Phe255 (Figure 5). This revealed different binding modes and potential molecular mechanisms underlying its interactions with LXR α in various heterodimeric contexts. Furthermore, we used the “dock” mode to calculate the binding affinity of compounds based on minimum energy values (kcal/mol) (Table 2). In both PDB IDs (1UHL and 2ACL), puniceloid D exhibited the lowest docking scores (−8.535 and −9.783 kcal/mol, respectively) and G scores (−8.841 and −10.098 kcal/mol, respectively) compared to oxepinamide K, indicating more stable binding conformations. This work provides more evidence that the quinazolinone skeleton is a useful model for the synthesis of LXR agonists.

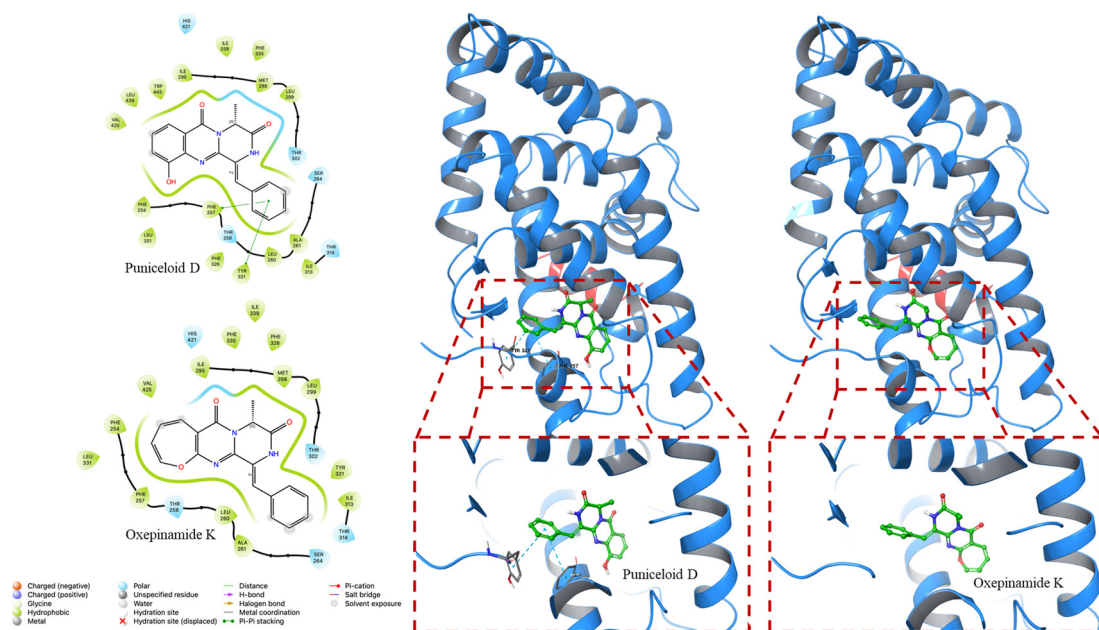


Figure 4. In silico docking study of puniceoloid D and oxepinamide K with LXR α of LXR α -RXR β LBD heterodimer (PDB ID: 1UHL). Puniceoloid D exhibited π - π stacking interactions with Phe257 and Tyr32.

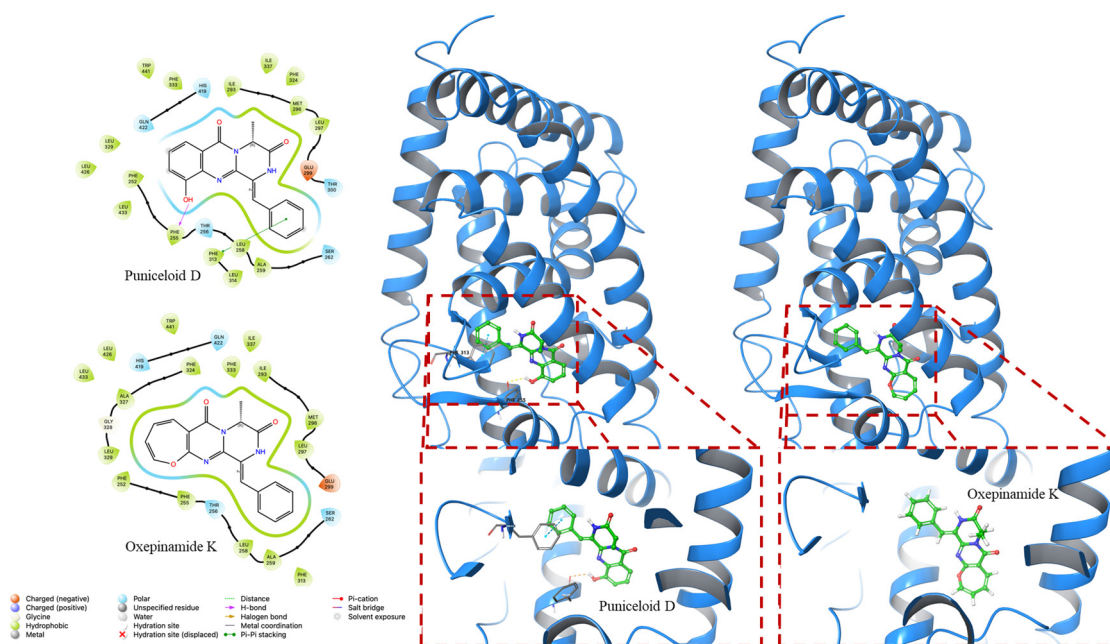


Figure 5. In silico docking study of puniceoloid D and oxepinamide K with LXR α of LXR α -RXR α LBD heterodimer (PDB ID: 2ACL). Puniceoloid D exhibited π - π stacking interactions with Phe313 and hydrogen bonding interactions with Phe255.

Table 2. Glide XP docking scores for puniceloid D and oxepinamide K with two LXR α LBD (PDB ID: 1UHL and 2ACL).

PDB ID	Compounds	Docking Score (Kcal/mol)	G Score (Kcal/mol)
1UHL	Puniceloid D	−8.535	−8.841
	Oxepinamide K	−8.113	−8.113
2ACL	Puniceloid D	−9.783	−10.089
	Oxepinamide K	−8.252	−8.252

4. Materials and Methods

4.1. Materials and Synthetic Methods

NMR spectra were acquired using Jeol JNM-ECX400 spectrometers (Jeol, Tokyo, Japan) operating at 400 MHz for ^1H and at 100 MHz for ^{13}C . Chemical shifts were reported in parts per million (ppm), and coupling constants were expressed in hertz (Hz). High-resolution mass spectra (HRMS) were obtained in positive mode using electrospray ionization (ESI-MS) with an Agilent 6530 accurate-mass quadrupole time-of-flight (Q-TOF) mass spectrometer (Agilent, Santa Clara, CA, USA). Biotage IsoleraTM (Uppsala, Sweden) was used for medium-pressure liquid chromatography (MPLC), and silica gel (ZEOprep 60, 40–63 μm , ZEOCHEM, Rüti, Switzerland) was utilized for column chromatography. A Kieselgel 60 F254 plate from Merck (Darmstadt, Germany) was used for thin-layer chromatography (TLC). The reagents and solvents utilized in this experiment were commercially available and used without any additional purification steps.

4.1.1. Synthesis of Ethyl (*tert*-Butoxycarbonyl)-*D*-alanyl-glycinate (7)

(*tert*-Butoxycarbonyl)-*D*-alanine (1.0 g, 5.3 mmol) was dissolved in anhydrous dichloromethane (DCM) (38 mL) in an ice bath. To the dissolved solution, 1-hydroxybenzotriazole (HOBt) (1.07 g, 7.93 mmol) and glycine ethyl ester hydrochloride (1.48 g, 10.6 mmol) were added. After 5 min, triethylamine (TEA) (3.32 mL, 23.8 mmol) was added dropwise, followed by the addition of 1-ethyl-3-[3-(dimethylamino)propyl]carbodiimide hydrochloride (EDC.HCl) (1524 mg, 7.93 mmol). The ice bath was then removed, and the reaction mixture was stirred at room temperature for 16 h. Upon completion of the reaction, the solution was diluted with DCM and washed with 1N HCl. Then, the combined organic layers were washed with a saturated NaHCO_3 solution. The aqueous layer was further extracted twice with DCM. Moisture was removed by passing the organic layer through anhydrous MgSO_4 and filtering. Purification was carried out using medium-pressure liquid chromatography (MPLC) with an elution solvent mixture of ethyl acetate and hexane in a ratio of 2:3, and compound 7 was obtained with a yield of 73.4%. Figure S1: ^1H NMR (400 MHz, CDCl_3) δ 6.63 (brs, 1H), 4.97 (brs, 1H), 4.21 (q, $J = 7.1$ Hz, 3H), 4.03 (m, 2H), 1.45 (s, 9H), 1.38 (d, $J = 7.4$ Hz, 3H), 1.28 (t, $J = 7.3$ Hz, 3H) [30]. Figure S2: ^{13}C NMR (100 MHz, CD_3OD) δ 176.4, 171.1, 157.6, 80.6, 62.2, 51.5, 42.0, 28.6, 18.4, 14.4.

4.1.2. Synthesis of (*R*)-3-methylpiperazine-2,5-dione (6)

Ethyl (*tert*-butoxycarbonyl)-*D*-alanyl-glycinate (7) (1.07 g, 3.89 mmol) was dissolved in dimethylformamide (DMF) (7.8 mL). Subsequently, 70.2 mL of water was added. The reaction solution was heated at 150 $^\circ\text{C}$ for 2 h and 30 min using a microwave. After completion of the reaction, methanol was added to the reaction mixture, and the solvent was concentrated using a rotary evaporator. The resulting material was then subjected to purification through silica gel filtration under the conditions of DCM and MeOH in a ratio of 95:5, and compound 6 was obtained with a yield of 60.8%. Figure S3: ^1H NMR (400 MHz, CD_3OD) δ 4.00 (q, $J = 7.0$ Hz, 1H), 3.90 (m, 2H), 1.41 (d, $J = 7.0$ Hz, 3H) [31]. Figure S4: ^{13}C NMR (100 MHz, CD_3OD) δ 171.6, 168.7, 51.6, 45.4, 19.4.

4.1.3. Synthesis of (*R*)-1,4-diacetyl-3-methylpiperazine-2,5-dione (5)

(*R*)-3-Methylpiperazine-2,5-dione (6) (303 mg, 2.36 mmol) and acetic anhydride (6.26 mL, 0.38 M) were combined and refluxed at 130 °C for 17 h. After completion of the reaction, acetic anhydride was removed by evaporating through a rotary evaporator, and the concentrated solution was purified using MPLC with an elution solvent mixture of ethyl acetate and hexane in a ratio of 1:3. Compound 5 was obtained with a yield of 81.3%. Figure S5: ¹H NMR (400 MHz, CD₃OD) δ 5.10 (q, *J* = 7.3 Hz, 1H), 4.20–4.96 (q, *J* = 18 Hz, 2H), 2.48 (s, 3H), 2.47 (s, 3H), 1.47 (d, *J* = 7.3 Hz, 3H) [39]. Figure S6: ¹³C NMR (100 MHz, CD₃OD) δ 172.8, 172.6, 170.4, 167.6, 55.4, 47.3, 27.0, 26.9, 17.6.

4.1.4. Synthesis of (*R,Z*)-1-acetyl-3-benzylidene-6-methylpiperazine-2,5-dione (4)

(*R*)-1,4-Diacetyl-3-methylpiperazine-2,5-dione (5) (405 mg, 1.92 mmol) was dissolved in dimethylformamide at 0 °C (5.05 mL), followed by the dropwise addition of benzaldehyde (0.502 mL, 2.56 eq). Subsequently, a 1 M solution of *t*-BuOK/*t*-BuOH (2.30 mL, 1.2 eq) was slowly added dropwise. After 5 min, the ice bath was removed, and the reaction mixture was stirred at room temperature for 18 h. Upon completion of the reaction, a saturated NH₄Cl solution was added to quench the reaction, followed by extraction three times with ethyl acetate. Moisture was removed using anhydrous MgSO₄, and the solvent evaporated. The resulting material was purified under the conditions of ethyl acetate and hexane in a ratio of 1:3. Compound 4 was obtained with a yield of 61.1%. Figure S7: ¹H NMR (400 MHz, CDCl₃) δ 7.85 (brs, 1H), 7.49–7.37 (m, 5H), 7.18 (s, 1H), 5.16 (q, *J* = 7.1 Hz, 1H), 2.61 (s, 3H), 1.57 (d, *J* = 7.1 Hz, 3H) [33]. Figure S8: ¹³C NMR (100 MHz, CDCl₃) δ 172.0, 167.1, 160.9, 132.6, 129.6, 129.6, 128.8, 125.7, 120.3, 52.8, 27.1, 20.0.

4.1.5. Synthesis of (*R,Z*)-3-benzylidene-6-methylpiperazine-2,5-dione (3)

(*R,Z*)-1-Acetyl-3-benzylidene-6-methylpiperazine-2,5-dione (4) (95.0 mg, 0.368 mmol) was dissolved in anhydrous methanol (6.69 mL). Hydrazine hydrate (0.0386 mL) was then added dropwise to the reaction mixture, resulting in the formation of a solid in the reaction solution. After the completion of the reaction, the product was purified through recrystallization, and compound 3 was obtained with a yield of 15.1%. Figure S9: ¹H NMR (400 MHz, DMSO-*d*₆) δ = 9.89 (brs, 1H), 8.45 (brs, 1H), 7.48 (d, *J* = 7.14 Hz, 2H), 7.38 (t, *J* = 7.86 Hz, 2H), 7.28 (t, *J* = 7.37 Hz, 1H), 6.81 (s, 1H), 4.10 (q, *J* = 6.9 Hz, 1H), 1.31 (d, *J* = 7.0 Hz, 3H) [40,41]. Figure S10: ¹³C NMR (100 MHz, DMSO-*d*₆) δ 167.7, 160.3, 133.4, 129.2, 128.6, 127.9, 127.0, 114.0, 50.3, 19.3.

4.1.6. Synthesis of (*R,Z*)-6-benzylidene-5-ethoxy-3-methyl-3,6-dihydropyrazin-2(1*H*)-one (2)

(*R,Z*)-3-Benzylidene-6-methylpiperazine-2,5-dione (3) (82.0 mg, 0.379 mmol) and Na₂CO₃ (241 mg, 2.27 mmol) were dissolved in anhydrous DCM (5.41 mL). Meerwein's salt (1 M, 1.2 eq)—dissolved in DCM—was then added, and the mixture was stirred at room temperature for 24 h. After the reaction was complete, ice was placed into the reaction vessel, and the resulting mixture was extracted three times with DCM. Moisture was removed through anhydrous MgSO₄, followed by filtration and evaporation. Purification was carried out through MPLC under the conditions of ethyl acetate and hexane in a ratio of 1:4. Compound 2 was obtained with a yield of 33.5%. Figure S11: ¹H NMR (400 MHz, CDCl₃) δ = 7.75 (s, 1H), 7.40 (d, *J* = 7.24 Hz, 2H), 7.33 (d, *J* = 6.84 Hz, 2H), 7.32 (m, 1H), 6.54 (s, 1H), 4.39 (q, *J* = 7.25 Hz, 1H), 4.27 (m, 2H), 1.55 (d, *J* = 7.27 Hz, 3H), 1.39 (t, *J* = 7.0 Hz, 3H). Figure S12: ¹³C NMR (100 MHz, CDCl₃) δ 173.1, 155.4, 134.7, 130.0, 129.8, 129.1, 124.5, 112.6, 63.2, 57.0, 21.5, 14.5.

4.1.7. Synthesis of Puniceloid D (1)

(*R,Z*)-6-Benzylidene-5-ethoxy-3-methyl-3,6-dihydropyrazin-2(1*H*)-one (2) (31.0 mg, 0.127 mmol) was dissolved in anhydrous acetonitrile (1.49 mL). Subsequently, 3-hydroxyanthranilic acid (25.3 mg, 0.165 mmol) was added, and the reaction was carried out at 200 °C for 2 h under microwave conditions. After evaporating the solvent, the product was

purified using ethyl acetate and hexane in a ratio of 1:2. The target compound (**1**) was obtained with a yield of 9.45%. Figure S13: ^1H NMR (400 MHz, $\text{DMSO-}d_6$) δ 10.56 (s, 1H), 9.76 (s, 1H), 7.71 (s, 1H), 7.66 (d, $J = 7.71$ Hz, 2H), 7.58 (dd, $J = 1.4, 7.9$ Hz, 1H), 7.47 (t, $J = 7.62$ Hz, 2H), 7.40–7.37 (m, 1H), 7.37 (t, $J = 7.9$ Hz, 1H), 7.26 (dd, $J = 1.4, 7.9$ Hz, 2H), 5.22 (q, $J = 6.8$ Hz, 1H), 1.49 (d, $J = 7.0$ Hz, 3H). Figure S14: ^{13}C NMR (100 MHz, CDCl_3) δ 166.3, 160.0, 151.7, 143.3, 135.6, 133.0, 129.7, 129.2, 128.6, 128.7, 125.9, 120.4, 117.8, 117.7, 116.3, 52.0, 19.5. HRMS (ESI, m/z): $[\text{M} + \text{H}]^+$ calculated for $\text{C}_{19}\text{H}_{15}\text{N}_3\text{O}_3$, 334.1191; found 334.1189.

4.2. Molecular Docking Experiment

The docking studies were conducted using Glide in Extra Precision (XP) employed by Schrödinger (version 2023-4). LXR α structures were acquired from the Protein Data Bank (PDB) with codes 1UHL and 2ACL [42]. The 2D structures of the compounds were obtained in .sdf file format using CS ChemDraw (version 20) and were subsequently converted into 3D structures. The ligands were independently docked into the energy-minimized structures of the ligand-binding domains (LBD) of LXR α . Docking scores and G scores were calculated to assess the binding of each tested compound with LXR α .

5. Conclusions

Diseases related to metabolic syndrome, such as obesity and diabetes, exhibit a concerning global prevalence, making them significant health priorities. The LXRs play a major role in regulating lipid and cholesterol metabolism, in addition to their anti-inflammatory activities. Natural products can act as both independent sources for novel drugs and foundational structures for drug discovery. In the present study, we pursued a seven-step synthetic pathway, starting from readily available and inexpensive starting materials, to accomplish the synthesis of the natural product puniceloid D—a novel and potent liver X receptor agonist. Furthermore, the molecular docking study revealed that puniceloid D exhibited favorable binding scores with two LXR α LBD structures (PDB ID: 1UHL and 2ACL) in comparison to oxepinamide K. Puniceloid D demonstrated a favorable conformational state, engaging in hydrogen bond and π – π stacking interactions within the active sites of LXR α . Promising natural products can be chemically modified to overcome their low yield and complicated synthetic pathways, thereby increasing their commercial potential. Our future research will explore the chemical modification of puniceloid D and investigating the mechanisms of action of its compounds would also be of interest.

Supplementary Materials: The following supporting information can be downloaded at: <https://www.mdpi.com/article/10.3390/molecules29020416/s1>, Figures S1–S14: ^1H NMR and ^{13}C NMR of compounds 1–7; Figure S15: Comparative NMR Data of **1** (A) and the reported one (B).

Author Contributions: Y.J.J., N.H., J.P., S.H., J.-K.J. and J.-H.K. designed the study. Y.J.J. and N.H. performed the experiments. Y.J.J., N.H. and J.-H.K. analyzed the experimental results. Y.J.J., N.H., J.P., S.H., J.-K.J. and J.-H.K. drafted the manuscript. N.H. and J.-H.K. finalized the manuscript. All authors have read and agreed to the published version of the manuscript.

Funding: This research was supported by the “Regional Innovation Strategy (RIS)” through the National Research Foundation of Korea (NRF), funded by the Ministry of Education (MOE) (2021RIS-001) and by the Ministry of Education of the Republic of Korea and the National Research Foundation of Korea (NRF-2023R1A2C1003659).

Institutional Review Board Statement: Not applicable.

Informed Consent Statement: Not applicable.

Data Availability Statement: All the data were provided in the main manuscript and Supplementary Materials.

Conflicts of Interest: The authors declare no conflicts of interest.

References

1. Hiebl, V.; Ladurner, A.; Latkolik, S.; Dirsch, V.M. Natural Products as Modulators of the Nuclear Receptors and Metabolic Sensors LXR, FXR and RXR. *Biotechnol. Adv.* **2018**, *36*, 1657–1698. [[CrossRef](#)] [[PubMed](#)]
2. Lee, E.K.; Park, Y.J. Metabolic Regulation of Nuclear Receptors. *J. Korean Endocr. Soc.* **2008**, *23*, 155–164. [[CrossRef](#)]
3. Degirolamo, C.; Sabbà, C.; Moschetta, A. Intestinal Nuclear Receptors in HDL Cholesterol Metabolism. *J. Lipid Res.* **2015**, *56*, 1262–1270. [[CrossRef](#)]
4. Gronemeyer, H.; Gustafsson, J.-Å.; Laudet, V. Principles for Modulation of the Nuclear Receptor Superfamily. *Nat. Rev. Drug Discov.* **2004**, *3*, 950–964. [[CrossRef](#)] [[PubMed](#)]
5. Wenzel, C.; Gödtke, L.; Reichstein, A.; Keiser, M.; Busch, D.; Drozdzik, M.; Oswald, S. Gene Expression and Protein Abundance of Nuclear Receptors in Human Intestine and Liver: A New Application for Mass Spectrometry-Based Targeted Proteomics. *Molecules* **2022**, *27*, 4629. [[CrossRef](#)]
6. Mangelsdorf, D.J.; Evans, R.M. The RXR Heterodimers and Orphan Receptors. *Cell* **1995**, *83*, 841–850. [[CrossRef](#)]
7. Chawla, A.; Repa, J.J.; Evans, R.M.; Mangelsdorf, D.J. Nuclear Receptors and Lipid Physiology: Opening the X-Files. *Science* **2001**, *294*, 1866–1870. [[CrossRef](#)]
8. Janowski, B.A.; Willy, P.J.; Devi, T.R.; Falck, J.R.; Mangelsdorf, D.J. An Oxysterol Signalling Pathway Mediated by the Nuclear Receptor LXR α . *Nature* **1996**, *383*, 728–731. [[CrossRef](#)]
9. Jamroz-Wiśniewska, A.; Wójcicka, G.; Horoszewicz, K.; Bełtowski, J. Liver X Receptors (LXRs). Part I: Structure, Function, Regulation of Activity, and Role in Lipid Metabolism. *Adv. Hyg. Exp. Med.* **2007**, *61*, 736–759.
10. Li, N.; Wang, X.; Zhang, J.; Liu, C.; Li, Y.; Feng, T.; Xu, Y.; Si, S. Identification of a Novel Partial Agonist of Liver X Receptor α (LXR α) via Screening. *Biochem. Pharmacol.* **2014**, *92*, 438–447. [[CrossRef](#)]
11. Smith, T.K.T.; Kahiel, Z.; LeBlond, N.D.; Ghorbani, P.; Farah, E.; Al-Awosi, R.; Cote, M.; Gadde, S.; Fullerton, M.D. Characterization of Redox-Responsive LXR-Activating Nanoparticle Formulations in Primary Mouse Macrophages. *Molecules* **2019**, *24*, 3751. [[CrossRef](#)] [[PubMed](#)]
12. Chen, M.; Yang, F.; Kang, J.; Gan, H.; Yang, X.; Lai, X.; Gao, Y. Identification of Potent LXR β -Selective Agonists without LXR α Activation by in Silico Approaches. *Molecules* **2018**, *23*, 1349. [[CrossRef](#)] [[PubMed](#)]
13. Repa, J.J.; Mangelsdorf, D.J. The Role of Orphan Nuclear Receptors in the Regulation of Cholesterol Homeostasis. *Annu. Rev. Cell Dev. Biol.* **2000**, *16*, 459–481. [[CrossRef](#)]
14. Apfel, R.; Benbrook, D.; Lernhardt, E.; Ortiz, M.A.; Salbert, G.; Pfahl, M. A Novel Orphan Receptor Specific for a Subset of Thyroid Hormone-Responsive Elements and Its Interaction with the Retinoid/Thyroid Hormone Receptor Subfamily. *Mol. Cell. Biol.* **1994**, *14*, 7025–7035. [[PubMed](#)]
15. Ni, M.; Zhang, B.; Zhao, J.; Feng, Q.; Peng, J.; Hu, Y.; Zhao, Y. Biological Mechanisms and Related Natural Modulators of Liver X Receptor in Nonalcoholic Fatty Liver Disease. *Biomed. Pharmacother.* **2019**, *113*, 108778. [[CrossRef](#)]
16. Maqdasy, S.; Trousson, A.; Tauveron, I.; Volle, D.H.; Baron, S.; Lobaccaro, J.-M.A. Once and for All, LXR α and LXR β Are Gatekeepers of the Endocrine System. *Mol. Aspects Med.* **2016**, *49*, 31–46. [[CrossRef](#)]
17. El-Gendy, B.E.-D.M.; Goher, S.S.; Hegazy, L.S.; Arief, M.M.H.; Burris, T.P. Recent Advances in the Medicinal Chemistry of Liver X Receptors: Miniperspective. *J. Med. Chem.* **2018**, *61*, 10935–10956. [[CrossRef](#)]
18. Komati, R.; Spadoni, D.; Zheng, S.; Sridhar, J.; Riley, K.E.; Wang, G. Ligands of Therapeutic Utility for the Liver X Receptors. *Molecules* **2017**, *22*, 88. [[CrossRef](#)]
19. Liang, X.; Zhang, X.; Lu, X.; Zheng, Z.; Ma, X.; Qi, S. Diketopiperazine-Type Alkaloids from a Deep-Sea-Derived *Aspergillus Puniceus* Fungus and Their Effects on Liver X Receptor α . *J. Nat. Prod.* **2019**, *82*, 1558–1564. [[CrossRef](#)]
20. He, L.; Li, H.; Chen, J.; Wu, X.-F. Recent Advances in 4 (3 H)-Quinazolinone Syntheses. *RSC Adv.* **2014**, *4*, 12065–12077. [[CrossRef](#)]
21. Mhaske, S.B.; Argade, N.P. The Chemistry of Recently Isolated Naturally Occurring Quinazolinone Alkaloids. *Tetrahedron* **2006**, *62*, 9787–9826. [[CrossRef](#)]
22. Michael, J.P. Quinoline, Quinazoline and Acridone Alkaloids. *Nat. Prod. Rep.* **2005**, *22*, 627–646. [[CrossRef](#)] [[PubMed](#)]
23. Avendano, C.; Menendez, J. Chemistry of Pyrazino [2, 1-b] Quinazoline-3, 6-Diones. *Curr. Org. Chem.* **2003**, *7*, 149–173. [[CrossRef](#)]
24. Park, J.; Nurkolis, F.; Won, H.; Yang, J.; Oh, D.; Jo, H.; Choi, J.; Chung, S.; Kurniawan, R.; Kim, B. Could Natural Products Help in the Control of Obesity? Current Insights and Future Perspectives. *Molecules* **2023**, *28*, 6604. [[CrossRef](#)] [[PubMed](#)]
25. Han, D.-G.; Cho, S.-S.; Kwak, J.-H.; Yoon, I.-S. Medicinal Plants and Phytochemicals for Diabetes Mellitus: Pharmacokinetic Characteristics and Herb-Drug Interactions. *J. Pharm. Investig.* **2019**, *49*, 603–612. [[CrossRef](#)]
26. Hosseini Nasab, N.; Shah, F.H.; Kim, S.J. Pharmacological Role of *Ostericum Koreanum*: A Short Viewpoint. *Nat. Prod. Commun.* **2021**, *16*, 1934578X211050790. [[CrossRef](#)]
27. Cledera, P.; Avendaño, C.; Menéndez, J.C. Comparative Study of Synthetic Approaches to 1-Arylmethylenepyrazino [2, 1-b] Quinazoline-3, 6-Diones. *Tetrahedron* **1998**, *54*, 12349–12360. [[CrossRef](#)]
28. Kim, J.; Movassaghi, M. Concise Total Synthesis and Stereochemical Revision of (+)-Naseseazines A and B: Regioselective Arylative Dimerization of Diketopiperazine Alkaloids. *J. Am. Chem. Soc.* **2011**, *133*, 14940–14943. [[CrossRef](#)]
29. Smeenk, J.M.; Ayres, L.; Stunnenberg, H.G.; van Hest, J.C.M. Polymer Protein Hybrids. *Macromol. Symp.* **2005**, *225*, 1–8. [[CrossRef](#)]
30. Mollica, A.; Davis, P.; Ma, S.-W.; Lai, J.; Porreca, F.; Hruby, V.J. Synthesis and Biological Evaluation of New Biphalin Analogues with Non-Hydrazine Linkers. *Bioorg. Med. Chem. Lett.* **2005**, *15*, 2471–2475. [[CrossRef](#)]

31. Coursindel, T.; Restouin, A.; Dewynter, G.; Martinez, J.; Collette, Y.; Parrot, I. Stereoselective Ring Contraction of 2, 5-Diketopiperazines: An Innovative Approach to the Synthesis of Promising Bioactive 5-Membered Scaffolds. *Bioorg. Chem.* **2010**, *38*, 210–217. [[CrossRef](#)] [[PubMed](#)]
32. Liao, S.; Qin, X.; Li, D.; Tu, Z.; Li, J.; Zhou, X.; Wang, J.; Yang, B.; Lin, X.; Liu, J. Design and Synthesis of Novel Soluble 2, 5-Diketopiperazine Derivatives as Potential Anticancer Agents. *Eur. J. Med. Chem.* **2014**, *83*, 236–244. [[CrossRef](#)]
33. Mollica, A.; Costante, R.; Fiorito, S.; Genovese, S.; Stefanucci, A.; Mathieu, V.; Kiss, R.; Epifano, F. Synthesis and Anti-Cancer Activity of Naturally Occurring 2, 5-Diketopiperazines. *Fitoterapia* **2014**, *98*, 91–97. [[CrossRef](#)] [[PubMed](#)]
34. Katritzky, A.R.; Fan, W.; Szajda, M.; Li, Q.; Caster, K.C. Conjugated Systems Derived from Piperazine-2, 5-dione. *J. Heterocycl. Chem.* **1988**, *25*, 591–597. [[CrossRef](#)]
35. Wang, Z. *Comprehensive Organic Name Reactions*; John Wiley & Sons, Inc.: Hoboken, NJ, USA, 2010; Volume 2.
36. Cledera, P.; Sanchez, J.D.; Caballero, E.; Yates, T.; Ramirez, E.G.; Avendano, C.; Ramos, M.T.; Menendez, J.C. Microwave-Assisted, Solvent-Free Synthesis of Several Quinazoline Alkaloid Frameworks. *Synthesis* **2007**, *21*, 3390–3398.
37. Argyrakis, W.; Köppl, C.; Werner, H.; Frey, W.; Baro, A.; Laschat, S. A Combined Quantum Mechanical and Experimental Approach towards Chiral Diketopiperazine Hydroperoxides. *J. Phys. Org. Chem.* **2011**, *24*, 682–692. [[CrossRef](#)]
38. Albers, M.; Blume, B.; Schlueter, T.; Wright, M.B.; Kober, I.; Kremoser, C.; Deuschle, U.; Koegl, M. A Novel Principle for Partial Agonism of Liver X Receptor Ligands: Competitive Recruitment of Activators and Repressors. *J. Biol. Chem.* **2006**, *281*, 4920–4930. [[CrossRef](#)]
39. Senbonmatsu, Y.; Kimura, S.; Akiba, M.; Ando, S.; Saito, N. Preparation of Chiral Right-Half Models of Antitumor Bistetrahydroisoquinolinequinone Natural Products. *Heterocycles* **2018**, *97*, 1050–1067.
40. Kanzaki, H.; Imura, D.; Nitoda, T.; Kawazu, K. Enzymatic Conversion of Cyclic Dipeptides to Dehydro Derivatives That Inhibit Cell Division. *J. Biosci. Bioeng.* **2000**, *90*, 86–89. [[CrossRef](#)]
41. Zhang, Q.; Li, S.; Chen, Y.; Tian, X.; Zhang, H.; Zhang, G.; Zhu, Y.; Zhang, S.; Zhang, W.; Zhang, C. New Diketopiperazine Derivatives from a Deep-Sea-Derived Nocardiopsis Alba SCSIO 03039. *J. Antibiot.* **2013**, *66*, 31–36. [[CrossRef](#)]
42. Nishioka, T.; Endo-Umeda, K.; Ito, Y.; Shimoda, A.; Takeuchi, A.; Tode, C.; Hirota, Y.; Osakabe, N.; Makishima, M.; Suhara, Y. Synthesis and in Vitro Evaluation of Novel Liver X Receptor Agonists Based on Naphthoquinone Derivatives. *Molecules* **2019**, *24*, 4316. [[CrossRef](#)] [[PubMed](#)]

Disclaimer/Publisher's Note: The statements, opinions and data contained in all publications are solely those of the individual author(s) and contributor(s) and not of MDPI and/or the editor(s). MDPI and/or the editor(s) disclaim responsibility for any injury to people or property resulting from any ideas, methods, instructions or products referred to in the content.